

TRENDS IN OZONE CONCENTRATIONS IN THE IBERIAN PENINSULA BY QUANTILE REGRESSION AND CLUSTERING

A. Monteiro^{*1}, A. Carvalho¹, I. Ribeiro¹, M. Scotto², S. Barbosa³, A. Alonso⁴, J. M. Baldasano^{5,6}, M. T. Pay⁵, A.I. Miranda¹, C. Borrego¹

¹CESAM & Department of Environment and Planning, University of Aveiro, Aveiro, Portugal

²Department of Mathematics, University of Aveiro, Aveiro, Portugal

³Center of Geophysics, IDL, University of Lisbon, Lisbon, Portugal

⁴Departamento de Estadística, Universidad Carlos III de Madrid, Spain

⁵Earth Science Department, Barcelona Supercomputing Center, Jordi Girona 29, Edificio Nexus II, Barcelona, Spain

⁶Environmental Modeling Lab, Technical University of Catalonia, Barcelona, Spain

*Corresponding author: A. Monteiro, e-mail: alexandra.monteiro@ua.pt; Tel: +351 234 370220, Fax: +351 234 370309

Abstract

In this paper, 10-years of ozone (O₃) hourly concentrations collected over the period 2000–2009 in the Iberian Peninsula (IP) are analyzed using records from 11 background sites. All the selected monitoring stations present an acquisition efficiency above 85%. The changes in tropospheric ozone over the Iberian Peninsula are examined by means of quantile regression, which allows to analyse the trends not only in the mean but in the overall data distribution. In addition, the ozone hourly concentrations records are clustered on the basis of their resulting distributions.

The analysis showed that high altitude stations (> 900 m) have higher background O₃ concentrations (~80 µg.m⁻³). The same magnitude of background O₃ concentrations is found in stations near the Mediterranean Sea. On the other hand, the rural stations near the Atlantic coast present lower background values (~50-60 µg.m⁻³) than those of Mediterranean influence. The two sub-urban stations exhibit the lowest background concentrations (~45 µg.m⁻³). The results of the quantile regression show a very distinct behaviour of the data distribution, the slopes for a fixed quantile are not the same over IP, reflecting the spatial dependence of O₃ trends. Hence the rate of temporal change is not the same for all parts of the data distribution, as implicitly assumed in ordinary regression. The lower quantile (percentile 5) presents higher rates of change than the middle (percentile 50) and the upper quantile (percentile 95). The clustering procedure reveals what has been already detected in the quantile regression. The station with highest rates of decrease on the O₃ concentrations (easternmost station of IP) is isolated and then other clusters are formed among the moderately positive/negative O₃ trends around the IP. The clustering procedure highlighted that the largest trends are found for the lower ozone O₃ values, with largest negative trend at the easternmost station of IP, and also in northern and mainland stations, and an opposite behaviour, with positive O₃ trends, is observed at the Atlantic coast stations.

41 **Keywords:** Iberian Peninsula; tropospheric ozone; spatial and temporal analysis; quantile
42 regression; cluster procedure

43

44 **1. INTRODUCTION**

45 Tropospheric ozone (O₃) is a key determinant of the atmospheric oxidation state and a major
46 constituent of photochemical smog which impacts air quality at urban and regional scale. The
47 production of elevated levels of O₃ at ground level is of particular concern because it is known
48 to have adverse effects on human health, vegetation, and a variety of materials (EA, 2010a).
49 There is a high interest in quantifying surface O₃ concentrations and associated trends, as they
50 serve to indirectly quantify the impacts of the anthropogenic precursor reductions and to
51 evaluate the effects of emission control strategies (Tang et al., 2006; Sicard et al., 2009).

52 There have been a few studies on the analysis of surface O₃ trends in different regions of Europe
53 (Brönnimann et al., 2002, Jenkin, 2008; Sicard et al., 2009). Over the Iberian Peninsula (IP)
54 where high surface O₃ concentrations are monitored each year from April to September (EEA,
55 2010b), several analyses of surface O₃ concentrations have been carried out. However, they
56 were limited to a single location restricted to a region of the IP and adopting an ordinary
57 regression approach or based on the median/mean and high percentile O₃ analysis (Gimeno et
58 al., 1999; Millán et al., 2002; Ribas and Peñuelas, 2004; Adame et al., 2008).

59 Observations from background monitoring stations have revealed that baseline surface O₃
60 concentrations in the northern hemisphere have been increasing over the past three decades
61 (Marenco et al., 1994), with average increases of approximately 0.5–2% per year at northern
62 mid-latitudes (Vingarzan, 2004). The observed increasing trend in baseline O₃ concentrations is
63 believed to be driven by emissions and processing of O₃ precursors on a global scale (Jaffe et
64 al., 2003; Honrath et al., 2004; Derwent et al., 2006, 2007). Although this hemispheric baseline
65 influences O₃ concentrations throughout the IP, the observed concentrations can be further
66 modified by processes occurring on regional- and local-scales, which can both increase and
67 decrease O₃ levels. Therefore such processes occurring on local, regional, and global scales
68 have an influence on whether O₃ air quality standards at a given location are achieved (Jenkin,
69 2008). Although the progressive control of O₃ precursors emissions -like volatile organic
70 compounds (VOC) and nitrogen oxides (NO_x)- within the European Community since the early
71 1990s (CEC, 1991) have influenced the magnitude of the O₃ regional- and local- scale effects
72 (Derwent et al., 2003; Jonson et al., 2005; Vautard et al., 2006), the observed O₃ trends is
73 determined from the net trend of the global-, regional- and local-scale effects, the relative
74 contributions of which can vary both spatially and temporally.

75 Anthropogenic emissions of the main air pollutants across Europe have decreased continuously
76 between 1990 and 2008 in Europe (EEA, 2010a). Reported European emissions of NO_x and
77 NMVOC have both decreased by 39% and 51%, respectively, since 2000. Concerning Spain

78 and Portugal, the O₃ precursor emissions have also been reduced, namely for NO_x (8% and 7%,
79 respectively) and NMVOC (21% and 34%, respectively).

80 The understanding of the O₃ budget and trends in the troposphere over the IP is required to (a)
81 properly identify the various mechanisms that contribute to the observed hourly average
82 concentration distribution; and to (b) develop and test models capable of simulating and
83 predicting atmospheric chemical and physical processes (Lefohn et al., 2008). It is also
84 important to characterize the changes in the distribution of hourly average O₃ concentrations
85 which provide (a) quantitative feedback on the effects of emission reductions on O₃
86 concentrations; (b) insights concerning the long-range transport of O₃ outside IP and possible
87 impacts of climate change; and (c) important information on which processes dominate during a
88 specific time of the year and which processes are more likely to influence particular portions of
89 the distribution (Oltmans et al., 2006).

90 Robust statistical procedures can be applied to investigate the spatial and temporal evolution of
91 the O₃ concentrations over a region from historical datasets. This study adopts the method
92 introduced by Barbosa et al. (2011) which combines quantile regression and clustering
93 procedures in order to better assess the spatial and the temporal evolution of the hourly O₃
94 measurements over the IP. On the one hand, quantile regression (Koenker and Hallock, 2001)
95 provides the rate of change not only in the mean, as in ordinary regression, but also in all parts
96 of the data distribution. In this sense, the quantile regression quantifies the variability structure
97 of the hourly O₃ concentrations and assesses the changes in the data distribution. On the other
98 hand, cluster analysis is an adequate procedure to spatially characterize the regional variability
99 on the O₃ data and it has been widely used in different analysis of environmental processes
100 (Alonso et al., 2006; Scotto et al., 2009; Barbosa et al., 2011; Carvalho et al., 2011).

101 This work focuses on investigating the temporal and spatial trends of the hourly surface O₃
102 concentrations at background environment over the IP for the last decade (2000-2009). The
103 remainder of this paper is laid out as follows. Section 2 discusses the O₃ concentrations acquired
104 at the background monitoring stations used in this study. Section 3 describes the application of
105 the quantile regression approach and the clustering procedure. Results are presented in Section
106 4. Finally, in Section 5 the results are discussed and main conclusions are summarized.

107

108 **2. O₃ DATA OVER THE IBERIAN PENINSULA**

109 A total of 11 O₃ monitoring stations within the IP are selected taking into account their
110 background influence and the efficiency data collection (> 85%) during the 10-years period
111 (2000-2009) as shown in Fig. 1 and Table 1. The spatial coverage is suitable over the IP, with
112 two stations located in Portugal and the remaining 9 stations located over Spain.

113

114

(Figure 1)

115

116

(Table 1)

117

118 Ambient O₃ concentrations are reported on an hourly basis and were obtained from the
119 Portuguese Air Quality Database (www.qualar.org) and the **EMEP monitoring network**
120 (www.emep.int).

121 Fig. 2 shows the distribution of hourly O₃ concentrations by year. Different groups of stations
122 can be distinguished in terms of background values (median) and minimum/peak values.

123

124

(Figure 2)

125

126 **High altitude stations (> 900 m) (CPB, VIZ and PEN) show high background concentration**

127 **(~80 µg.m⁻³) due to higher O₃ levels in elevated terrains.** The same range of background O₃

128 concentrations are found in stations near the Mediterranean Sea (CCR, ZAR, and TOR). O₃

129 atmospheric dynamics in the Spanish Mediterranean areas is affected by mesoscale and local

130 meteorological processes but also regional factors, such as (Baldasano et al., 1994, Millán et al.,

131 1997; Toll and Baldasano, 2000; Martin-Vide and Olcina, 2001; Soriano et al., 2001; Pérez et

132 al., 2004): (1) the influence of the Azores high-pressure system, (2) the costal ranges

133 surrounding the Mediterranean coast, (3) the influence of the Iberian and Saharan thermal lows

134 causing weak pressure gradients over the Mediterranean (4) the intense breeze action along the

135 Mediterranean coast favoured by the prevailing low advective conditions, (5) the scarce summer

136 precipitation, and (6) the intense seasonal contrast concerning temperature, humidity and

137 rainfall. All these facts favour the photochemical formation of O₃ and contribute to the

138 accumulation and recirculation of aged air masses which contain O₃. The two rural stations

139 closest to Portugal and located under 506 m of altitude –BAR and SEV – register lower median

140 (~50-60 µg.m⁻³) than those of Mediterranean influence, also presenting O₃ peaks (P95) less than

141 **120 µg.m⁻³.** The NIB station, in the northern IP, also presents low median concentrations along

142 **the decade (~50-60 µg.m⁻³) due to the influence of large plumes coming from power plants**

143 **located in northeaster Spain (Pay et al., 2011) containing high NO_x concentration that affects O₃**

144 **chemistry in this region.** Such episodes happen under the influence of westerly winds which are

145 relatively frequent (Jorba et al., 2004). The two suburban stations (CUS and PP) exhibit the

146 lowest median (~45 µg.m⁻³) and the minimum O₃ concentrations (P5) (~ 0 µg.m⁻³), explained by

147 the O₃ destruction by NO (emitted by road-traffic and shipping in the urban and suburban areas

148 of Oporto and Lisbon) mainly at night-time (Seinfeld and Pandis, 1998).

149 During the study period the most critical years in terms of O₃ peaks/episodes were 2005 and

150 2006 for the majority of the stations. The summer period of these two years was characterized

151 by meteorological conditions very favourable for photochemical activity (Monteiro et al., 2005,

152 2007). The year 2003 was also a particular critical year in terms of photochemical activity (and
153 high O₃ values) due to the occurrence of a strong heat wave over the IP (Ordonez et al., 2010).

154

155 3. STATISTICAL METHODS

156 Quantile regression is a well-defined statistical technique for regression on quantiles rather than
157 regression on the mean. Although it was first introduced in econometrics by Koenker and Basset
158 (1978), quantile regression is being applied in various geoscience contexts (e.g. Koenker and
159 Schorfheide, 1994; Cade and Noon, 2003; Baur et al., 2004; Elsner et al., 2008; Barbosa et al.,
160 2011). We outline here the essential of the quantile regression approach. The starting point is a
161 random variable Y with cumulative continuous distribution function $F_Y(y)$ (by definition: $F_Y(y)$
162 $= P(Y \leq y)$). The quantile τ is defined as the value $Q_Y(\tau)$ such that $P(Y \leq Q_Y(\tau)) = \tau$, for $0 \leq \tau \leq 1$.
163 The quantile function $Q_Y(\tau)$ is defined from the cumulative distribution function $F_Y(y)$ as $Q_Y(\tau)$
164 $= F_Y^{-1}(\tau)$. Then considering the conditional distribution of Y given $X=x$, the conditional quantile
165 function $Q(Y|X)(\tau|x)$ verifies $P(Y \leq Q(Y|X)(\tau|x)|X=x) = \tau$. Whereas ordinary regression is based
166 on the conditional mean function $E(Y|X)=x$ and minimization of the respective residuals,
167 quantile regression is based on the conditional quantile function and minimization of the sum of

168 asymmetrically weighted absolute residuals $\sum_{i=1}^n \rho(\tau)(y_i - Q_{Y|X}(\tau|x_i))$, where $\rho(\cdot)$ represents
169 the tilted absolute value function. For further details see Koenker (2005).

170 The time series clustering procedure proposed to classify the time series of O₃ hourly
171 concentrations based on the corresponding distributions for quantile slopes at lower, middle and
172 upper quantiles is as follows: firstly, for a fixed (but arbitrary) quantile, the algorithm starts with
173 the estimation of the distribution corresponding to quantile slope estimates; second, the
174 corresponding *dissimilarity* matrix is computed. To this extend, an adequate metric between
175 univariate distribution functions is required. In the present setting the weighted L2-Wasserstein
176 distance between two quantile slope distributions is adopted. Finally, a dendrogram based on the
177 application of classical cluster techniques to the dissimilarity matrix is built and that provides
178 the different clusters formed by the distributions of the quantile slopes. In particular,
179 agglomerative hierarchical methods with nearest distance (single linkage), furthest distance
180 (complete linkage) and unweighted average distance (average linkage) are used as grouping
181 criteria. In order to summarise those distributions, the average linkage procedure is applied to
182 obtain dendrograms of slopes for quantiles 0.05, 0.5 and 0.95. Similar conclusions are obtained
183 using the single linkage and the complete linkage methods.

184

185 4. RESULTS

186 In this section, quantile regression is applied for the hourly O₃ concentrations in order to
187 describe the temporal variability of different quantiles of the O₃ distribution over IP. The

188 quantile slopes and corresponding standard errors are derived using the algorithm of Koenker
189 and D'Orey (1987). The clustering procedure is also discussed.
190 The results for all the stations are shown in Fig. 3, along with the quantile slopes at quantiles
191 0.05, 0.5 and 0.95, corresponding respectively to the lowest 5%, 50% (median) and 95% of the
192 ordered observations.

193
194 (Figure 3)
195

196 Several O₃ trends over the last decade can be identified in this group of stations. A significant
197 negative trend is only exhibited by CCR station, especially for lowest quantiles (P5). The same
198 tendency was found by Ribas and Peñuelas (2004) for a coastal station (Begur) in northeastern
199 Spain. CCR is a coastal station located in the northeastern extreme of the IP. This site presents
200 strong north-westerly winds (tramontane and mistral) channelled by Pyrenees and Central
201 Massif throughout the Gulf of Lyon. The flow crosses the Carcasone gap into the Mediterranean
202 which can transport new pollutants into the area that are added to local emissions and re-
203 circulated within the coastal breezes at eastern Iberian (Gangoiti et al., 2001). CPB, PEN –
204 located in the northern Spanish plateau – and SEV show a slightly negative slope, mainly for the
205 lower quantiles. BAR and ZAR monitoring sites don't show any significant trend for the three
206 quantiles.

207 By contrast, the NIB coastal station in the northern IP presents the largest positive trends, even
208 larger for lower concentration (P5). Similar trends are found in TOR and VIZ, sited under the
209 Mediterranean influence, and in a lesser extend at the two suburban stations at Oporto and
210 Lisbon cities (CUS and PP, respectively).

211 A more complete description of the quantile regression results is displayed in Fig. 4 which
212 displays the quantile slopes and the corresponding standard errors computed for quantiles 0.1 to
213 0.9 in steps of 0.02.

214
215 (Figure 4)
216

217 Fig. 4 clearly shows a distinct pattern for the different monitoring sites. However, there are
218 similarities between specific stations in terms of the sign and the distribution over the different
219 quantiles. CCR shows the highest negative slopes over all the analysed sites (from -28 to -19
220 $\mu\text{g}\cdot\text{m}^{-3}/\text{decade}$), with a higher decrease observed for the lower quantiles. A negative slope over
221 the all ranges of concentrations is also registered for the north mainland stations - CPB, SEV
222 and PEN - with similar magnitudes (around -5 and -10 $\mu\text{g}\cdot\text{m}^{-3}/\text{decade}$) of the quantile
223 distribution pattern. A slight negative slope ($> -2.5 \mu\text{g}\cdot\text{m}^{-3}/\text{decade}$) is also verified for ZAR and
224 BAR, but only for the lower quantiles.

225 On the opposite, the Atlantic coastal stations - NIB, CUS and PP - have positive slopes over the
226 all concentrations range with the lower increasing at a much faster rate than the middle and
227 upper values. Besides a similar quantile distribution, the magnitude of the slope is significantly
228 different, higher for NIB ($> 18 \mu\text{g}\cdot\text{m}^{-3}/\text{decade}$) and lower for CUS and PP ($\sim 5\text{-}15 \mu\text{g}\cdot\text{m}^{-3}/\text{decade}$),
229 $^3/\text{decade}$). Positive slopes are also found for the VIZ and TOR stations ($4\text{-}12 \mu\text{g}\cdot\text{m}^{-3}/\text{decade}$),
230 both presenting specific and unique quantile distribution.

231 For all cases the derived slopes vary with the quantiles and are distant to the original ordinary
232 least squares slope, indicating that the distribution of the ozone values is not symmetric and the
233 rate of change is not the same for all parts of the data distribution (lower, middle and upper
234 quantiles behave differently).

235 In summary over the last decade a group of stations – CCR, CPB, ZAR, BAR, SEV and PEN –
236 registered a decrease mainly on the lower quantiles of O_3 data distribution which reflect the
237 minimum (nocturnal) values over these areas. On the opposite, the rest of the monitoring sites –
238 NIB, PP, CUS, TOR and VIZ – exhibit a high positive slope on these lower quantiles, indicating
239 an increase over the background values of ozone.

240 Furthermore, the results of the clustering procedure, together with the spatial representation of
241 the quantile slopes, are shown in Fig. 5.

242

243 (Figure 5)

244

245 The dendrogram for the lower quantile (P5) clearly discriminates three groups: stations with
246 larger negative slopes, $\cong - 28 \mu\text{g}\cdot\text{m}^{-3}/\text{decade}$ (CCR), slight negative slopes (BAR, SEV, CPB,
247 PEN and ZAR) and the remaining stations with positive slopes (NIB, PP, CUS, TOR, VIZ).
248 These results corroborate the previous analysis, namely in what concerns the different trend on
249 the background ozone values registered over Iberian Peninsula. The second cluster, with
250 positive slopes, further distinguishes the station with the highest slope, $> 18 \mu\text{g}\cdot\text{m}^{-3}/\text{decade}$
251 (NIB) from the other stations. The third cluster, with negative slopes, further subdivides into
252 sites with moderate slopes and stations with very small or non-significant trends (BAR). A
253 similar pattern is found in the dendrogram for the median quantile (P50), with the same groups
254 identified.

255 The dendrogram for the upper quantile (P95) continues to distinguish the CCR station with the
256 highest negative slopes, $> -20 \mu\text{g}\cdot\text{m}^{-3}/\text{decade}$. Within the remaining stations, and differing from
257 the previous dendograms, the major subdivision clusters include (1) the rural stations with
258 positive trend (TOR, NIB and VIZ) and (2) all the other stations with negative slopes and the
259 two suburban stations. This last cluster is then subdivided into two clusters of slight/moderate
260 slopes (ZAR, CUS, BAR and PP) and a cluster of stations with high absolute negative slopes,
261 typically $< - 4 \mu\text{g}\cdot\text{m}^{-3}/\text{decade}$ (SEV, PEN and CPB).

262

263 5. DISCUSSION AND CONCLUSIONS

264 Quantile regression and clustering analysis are applied to study changes in hourly O₃ data over
265 the Iberian Peninsula on the last decade (2000-2009). Ozone data was collected from 11
266 background monitoring stations, spatially distributed along the IP, characterized by different
267 background values that goes from 30 µg.m⁻³ (suburban stations on the coast of Portugal) to 80
268 µg.m⁻³ (stations located in centre and east of IP).

269 Quantile regression allows computing trends at different quantiles of the O₃ data distribution
270 within a well-defined statistical framework. In addition, the classical clustering procedure
271 allows summarising the resulting distributions of sample quantile slopes. As in ordinary
272 regression, the slopes for a fixed quantile are not the same over IP, reflecting the spatial
273 dependence of O₃ trends. The results for all monitoring sites show different slopes for the 5%,
274 50% and 95% percentiles, indicating a different rate of temporal change for all parts of the data
275 distribution, as implicitly assumed in ordinary regression. Lower (P5), middle (P50) and upper
276 (P95) quantiles behave differently, with the lower quantiles of O₃ data distribution
277 increasing/decreasing at a much faster rate than the middle and higher quantiles.

278 For example, the CCR station located in the eastern extreme of IP, under influence of different
279 climatic patterns and topographic features, exhibit a very distinct behaviour, with a strong
280 negative trend (< -20 µg.m⁻³/decade) over all the data distribution, with a higher decrease
281 observed for the lower quantiles (background values) (~ -28 µg.m⁻³/decade). CPB, SEV and
282 PEN – located in the interior north part of IP – show a slight negative slope mainly for the lower
283 quantiles (-10 µg.m⁻³/decade). On the other hand, a positive slope (8-18 µg.m⁻³/decade) can be
284 identified for the stations – NIB, CUS and PP – sited over the Atlantic Ocean coast and also
285 TOR and VIZ (4-12 µg.m⁻³/decade), sited over the Mediterranean influence, and mainly on the
286 lower quantiles of O₃ data distribution (background values). This larger trend in the lower
287 quantiles than in the central and upper part of the data distribution was not found in studies
288 conducted over North America where higher hourly average O₃ concentrations decrease faster
289 than the mid- and lower-values (Lefohn et al., 2008).

290 The analysis of the clusters for different quantiles reflects the differences existent mainly
291 between the lower/middle and the upper quantile. The dendrograms for the lower and median
292 clearly discriminate three groups: stations with larger negative slopes (CCR), slight negative
293 slopes (BAR, SEV, CPB, PEN and ZAR) and the remaining stations with positive slopes (NIB,
294 PP, CUS, TOR, VIZ). The dendrogram for the upper quantile displays a distinct picture:
295 continues to distinguish the CCR station with the highest negative slopes, but the remaining
296 stations are classified in several sub-clusters with minor significance. In fact, the minor gradient
297 of spatial variability occurs at the 95% quantile, with slopes ranging from -8 µg.m⁻³/decade to 8
298 µg.m⁻³/decade.

299 In summary, this complementary analysis pointed out that the largest trends are found for the
300 lower O₃ values, with the largest negative trend at the easternmost station of the IP (CCR), and
301 also in northern and mainland stations (BAR, SEV, CPB and PEN), and an opposite behaviour
302 is detected at the Atlantic coastal stations (NIB, CUS and PP) with positive O₃ trends.

303

304 **ACKNOWLEDGEMENTS**

305 The authors gratefully acknowledge the Portuguese ‘Ministério da Ciência, da Tecnologia e do
306 Ensino Superior’ for the BIOAIR (PTDC/AAC-AMB/103866/2008) project, for the Ph.D
307 grant of Isabel Ribeiro (SFRH/ BD/60370/2009) and the post-doc grant of Alexandra Monteiro
308 (SFRH/BPD/63796/2009). The acknowledge is extended to the CRUP and the Ministerio de
309 Ciencia e Innovación of Spain by the support of the Integrated Action E 122-10/PT2009-0029.
310 The Spanish Ministry of Science and Innovation is also thanked for the Formación de Personal
311 Investigador (FPI) doctoral fellowship held by María Teresa Pay (CGL2006-08903).

312

313 **REFERENCES**

314 Adame J.A., Lozano A., Bolívar J.P., De la Morena B.A., Conteras J., Godoy F., 2008.
315 Behavior, distribution and variability of surface ozone at an arid region in the south of Iberian
316 Peninsula (Sevilla, Spain). *Chemosphere* 70, 841-849.

317 Alonso A.M., Berrendero JR, Hernández A, Justel A., 2006. Time series clustering based on
318 forecast densities. *Comput. Statist. Data Anal.*, 51 (2), 762-776.

319 Baldasano J.M., Cremades L., Soriano C., 1994. Circulation of air pollutants over the Barcelona
320 geographical area in summer. Proceedings of Sixth European Symposium Physic-Chemical
321 Behaviour of Atmospheric Pollutants. Varese, Italy, 18-22 October. Report EUR 15609/1 EN:
322 474-479.

323 Barbosa S.M., Scotto M.G., Alonso A.M., 2011. Summarising changes in air temperature over
324 central Europe by quantile regression and clustering. *Nat. Hazards Earth Syst. Sci.* (in press).

325 Baur D., Saisana M., Schulze N., 2004. Modelling the effects of meteorological variables on
326 ozone concentration – a quantile regression approach. *Atmos. Environ.*, 38, 4689-4699.

327 Brönnimann S., Buchmann B., Wanner H., 2002. Trends in near-surface ozone concentrations
328 in Switzerland: the 1990s. *Atmos. Environ.*, 36, 2841-2852.

329 Cade B., Noon B., 2003. A Gentle introduction to quantile regression for ecologists. *Frontiers in*
330 *Ecology and the Environment*, 1, 412-420.

331 Carvalho A.C., Carvalho A., Martins H., Marques C., Rocha A., Borrego C., Viegas D.X.,
332 Miranda A.I. (2011). Fire weather risk assessment under climate change using a dynamical
333 downscaling approach. *Environmental Modelling and Software* 26 (9), 1123-1133.

334 CEC, 1991, Commission of the European Communities CEC, 1991. Council directive amending
335 directive 70/220/EEC on the approximation of the laws of member states relating to the
336 measures to be taken against air pollution by emissions from motor vehicles. 91/441/EEC.
337 *Journal of the European Communities*, L242/1-L242/106.

338 Derwent R., Jenkin M., Saunders S., Pilling M., Simmonds, P., Passant, N., Dollard, G.,
339 Dumitrean P., Kent A., 2003. Photochemical ozone formation in north west Europe and its
340 control. *Atmos. Environ.*, 37, 1983–1991.

341 Derwent R.G., Simmonds P.G., O’Doherty S., Stevenson D.S., Collins W.J., Sanderson M.G.,
342 Johnson C.E., Dentener F., Cofala J., Mechler R., Amann M., 2006. External influences on
343 Europe’s air quality: baseline methane, carbon monoxide and ozone from 1990 and 2030 at
344 Mace Head, Ireland. *Atmos. Environ.*, 40, 844–855.

345 Derwent R.G., Simmonds P.G., Manning A.J., Spain T.G., 2007. Trends over a 20-year period
346 from 1987 to 2007 in surface ozone at the atmospheric research station, Mace Head, Ireland.
347 *Atmos. Environ.*, 41, 9091–9098.

348 EEA, 2010a. The European Environment. State and outlook 2010. Air pollution. European
349 Environmental Agency. Luxembourg, Publication Office of the European Union. ISBN 978-92-
350 9213-152-4. doi: 10.2800/57792.

351 EEA, 2010b. Air pollution by ozone across Europe during summer 2009. Overview of
352 exceedances of EC ozone threshold values for April-September 2009. Technical Report 2/2010.
353 European Environmental Agency.

354 Elsner J.B., Kossin J.P., Jagger T.H., 2008. The increasing intensity of the strongest tropical
355 cyclones. *Nature* 455, 92-95.

356 Gangoiti G., Millán M.M., Salvador R., Mantilla E., 2001. Long-range transport and re-
357 circulation of pollutants in the western Mediterranean during the project Regional Cycles of Air
358 Pollutions in the West-Central Mediterranean Area. *Atmos. Environ.*, 35, 6267-6276.

359 Gimeno L., Hernández E., Rúa A., García R., Martín I., 1999. Surface ozone in Spain.
360 *Chemosphere*, 38, 3061-3074.

361 Honrath R.E., Owen R.C., Val Martin M., Reid J.S., Lapina K., Fiahlo P., Dziobak M.P.,
362 Kleissel J., Westphal D.L., 2004. Regional and hemispheric impacts of anthropogenic and
363 biomass burning emissions on summertime CO and O₃ in the North Atlantic lower free
364 troposphere. *J. Geophys. Res.*, 109, D24310.

365 Jaffe D., Price H., Parrish D., Goldstein A., Harris J., 2003. Increasing background ozone during
366 spring on the west coast of North America. *Geophys. Res. Lett.*, 30(12), 1613,
367 doi:10.1029/2003GL017024.

368 Jenkin M., 2008. Trends in ozone concentration distributions in the UK since 1990: Local,
369 regional and global influences. *Atmos. Environ.*, 42, 5434–5445.

370 Jorba, O., Pérez, C., Rocadenbosch, F., Baldasano, J. M., 2004. Cluster Analysis of 4-Day Back
371 Trajectories Arriving in the Barcelona Area, Spain, from 1997 to 2002. *Journal of Applied*
372 *Meteorology*, 43(6), 887-901.

373 Jonson J. E., Simpson D., Fagerli H., Solberg S., 2005. Can we explain the trends in European
374 ozone levels? *Atmos. Chem. Phys.*, 6, 51– 66.

375 Koenker R., 2005. *Quantile regression*. Cambridge University Press, New York.

376 Koenker R., Basset G., 1978. Regression quantiles. *Econometrica*, 46, 33-50.

377 Koenker R., D'Orey V., 1987. Computing regression quantiles. *Applied Statistics*, 36, 383-393.

378 Koenker R., Schorfheide F., 1994. Quantile spline models for global temperature change.
379 *Climatic Change*, 28, 395-404.

380 Koenker R., Hallock, K., 2001. Quantile Regression. *Journal of Economic Perspectives*, 15,
381 143–156.

382 Lefohn A., Shadwick D., Oltmans S., 2008. Characterizing long-term changes in surface ozone
383 levels in the United States (1980–2005). *Atmos. Environ.*, 42, 8252–8262.

384 Martín-Vide J., Olcina J., 2001. *Climas y tiempos de España*. Ed. Alianza, Madrid, 258 pp.

385 Marengo A., Gouget H., Nedelec P., Pages J.-P., 1994. Evidence of a long term increase in
386 tropospheric ozone from Pic du Midi data series: Consequences: positive radiative forcing. *J.*
387 *Geophys. Res.*, 99, 16617-16632.

388 Millán M.M., Salvador R., Mantilla E., 1997. Photooxidant dynamics in the Mediterranean
389 basin in summer: Results from European research projects. *J. Geophys. Res.*, 102(D7), 8811-
390 8823.

391 Millán M., Sanz M.J., Salvador R., Mantilla, E., 2002. Atmospheric dynamics and ozone cycles
392 related to nitrogen deposition in the western Mediterranean. *Environ. Poll.*, 118, 167-186.

393 Monteiro, A., Vautard, R., Borrego, C., Miranda, A.I., 2005. Long-term simulations of photo
394 oxidant pollution over Portugal using the CHIMERE model. *Atmos. Environ.*, 39, 3089-3101.

395 Monteiro, A., Miranda, A.I., Borrego, C., Vautard, R., 2007. Air quality assessment for
396 Portugal. *Science of the Total Environment* 373, 22-31.

397 Oltmans S.J., Lefohn A.S., Harris J.M., Galbally I., Scheel H.E., Bodeker G., Brunke E., Claude
398 H., Tarasick D., Johnson B.J., Simmonds P., Shadwick D., Anlauf K., Hayden K., Schmidlin F.,
399 Fujimoto T., Akagi K., Meyer C., Nichol S., Davies J., Redondas A., Cuevas E., 2006. Long-
400 term changes in tropospheric ozone. *Atmos. Environ.*, 40 (17), 3156-3173.

401 Ordonez C., Elguindi N., Stein O., Huijnen V., Flemming J., Inness A., Flentje H., Katragkou
402 E., Moinat P., Peuch V., Segers A., Thouret V., Athier G., van Weele M., Zerefos C., Cammas
403 J., Schultz M., 2010. Global model simulations of air pollution during the 2003 European heat
404 wave. *Atmos. Chem. Phys.*, 10, 789–815.

405 Pay, M.T., Jiménez-Guerrero, P., Jorba, O., Basart, S., Pandolfi, M., Querol, X., Baldasano,
406 J.M., 2011. Spatio-temporal variability of levels and speciation of particulate matter across
407 Spain in the CALIOPE modeling system. Submitted in *Atmos. Environ.*

408 Pérez C., Sicard M., Jorba O., Comerón A., Baldasano J.M., 2004. Summertime re-circulations
409 of air pollutants over the north-eastern Iberian coast observed from systematic EARLINET lidar
410 measurements in Barcelona. *Atmos. Environ.*, 38, 3983-4000.

411 Ribas A., Peñuelas J., 2004. Temporal patterns of surface ozone levels in different habitats of
412 the north western Mediterranean basin. *Atmos. Environ.*, 38, 985-992.

413 Scotto M.G., Barbosa S.M., Alonso A.M., 2009. Model-based clustering of Baltic sea-level.
414 *Appl. Ocean Res.*, 31, 4-11.

415 Seinfeld J.H., Pandis S.N., 1998. *Atmospheric Chemistry and Physics: From air pollution to
416 climate change.* John Wiley & Sons, New York. ISBN: 9780471178163.

417 Sicard P., Coddeville P., Galloo J., 2009. Near-surface ozone levels and trends at rural stations
418 in France over the 1995-2003 period. *Environ. Monit. Assess.*, 156, 141-157.

419 Soriano C., Baldasano J.M., Buttler W.T., Moore K., 2001. Circulatory patterns of air pollutants
420 within the Barcelona air basin in a summertime situation: lidar and numerical approaches.
421 *Bound.-Lay. Meteorol.*, 98, 33-55.

422 Tang G., Li X., Wang Y., Xin J., Ren X., 2006. Surface ozone trend details and interpretations
423 in Beijing, 2001–2006. *Atmos. Chem. Phys.*, 9, 8813-8823.

424 Toll I., Baldasano J.M., 2000. Modeling of photochemical air pollution in the Barcelona area
425 with highly disaggregated anthropogenic and biogenic emissions. *Atmos. Environ.*, 34, 3060-
426 3084.

427 Vautard R., Szopa S., Beekmann M., Menut L., Hauglustaine D. A., Rouil L., Roemer M., 2006.
428 Are decadal anthropogenic emission reductions in Europe consistent with surface ozone
429 observations?, *Geophys. Res. Lett.*, 33, L13810, doi:10.1029/2006GL026080.

430 Vingarzan R., 2004. A review of surface ozone background levels and trends. *Atmos. Environ.*,
431 38, 3431-3442.

432

433

434 **Table captions**

435 Table 1. Selected O₃ background monitoring stations over the IP.

436

437

438 **Figure captions**

439

440 Figure 1. Map of the IP showing the locations of the background monitoring stations considered
441 in the present analysis (Table 1). The bullet size indicates the altitude and the round/square
442 shape the type of the background station (rural/suburban).

443

444 Figure 2. Whisker plots of the hourly O₃ concentrations, measured at the selected sites over the
445 IP, depicting the median (P50), the P5-P95 range and the non-outliers range.

446

447 Figure 3. Time series of hourly O₃ concentrations changes per decade ($[\mu\text{g}\cdot\text{m}^{-3}]/\text{decade}$) (solid
448 grey line) and trends for quantiles 0.05 (dashed line), 0.5 (solid line) and 0.95 (dotted line).

449

450 Figure 4. Quantile slopes (O₃ concentration $[\mu\text{g}\cdot\text{m}^{-3}]/\text{decade}$) and corresponding standard errors
451 for the selected group of stations. The horizontal dashed line represents the usual ordinary least
452 squares slope.

453

454 Figure 5. Dendrogram for 5%, 50% and 95% quantile slopes (right) and the spatial
455 representation of the quantile slopes (left).

456

Figure1

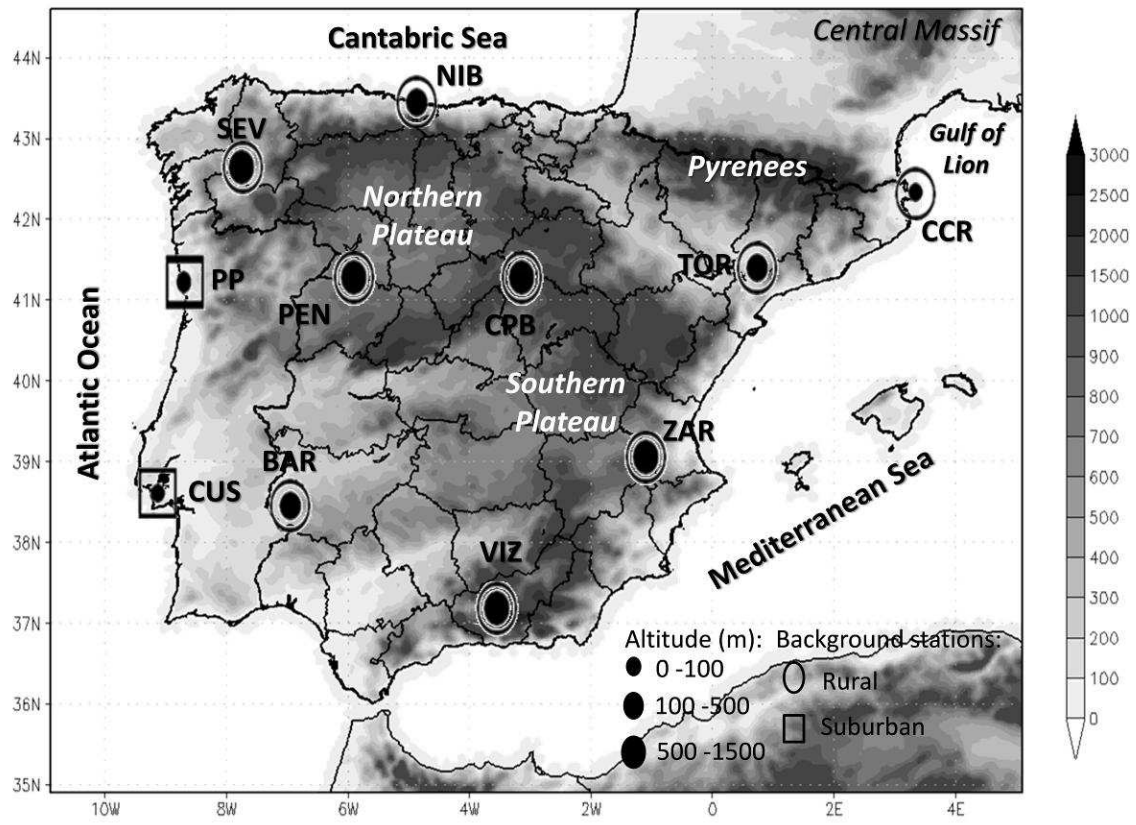


Figure2

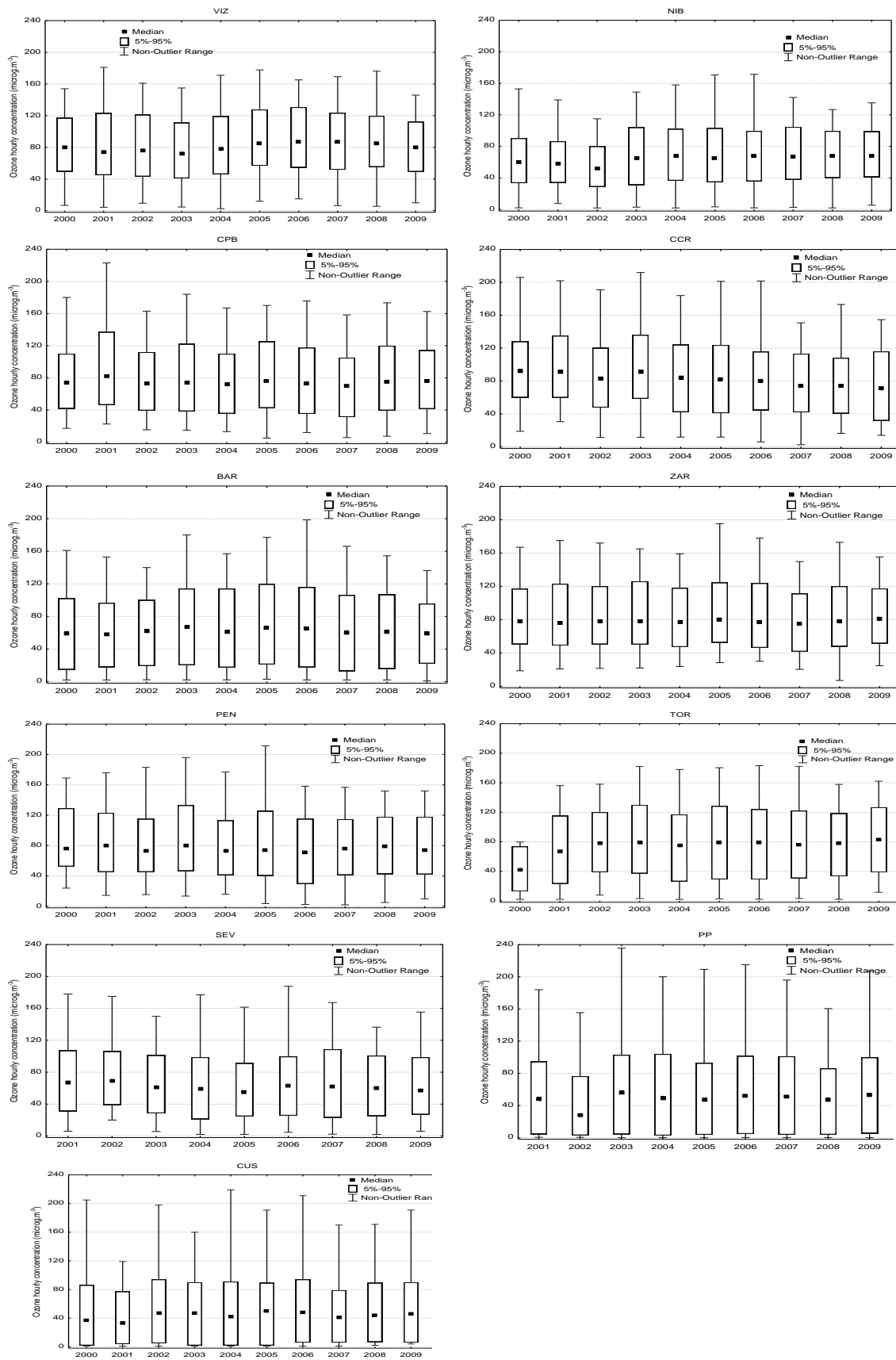


Figure3

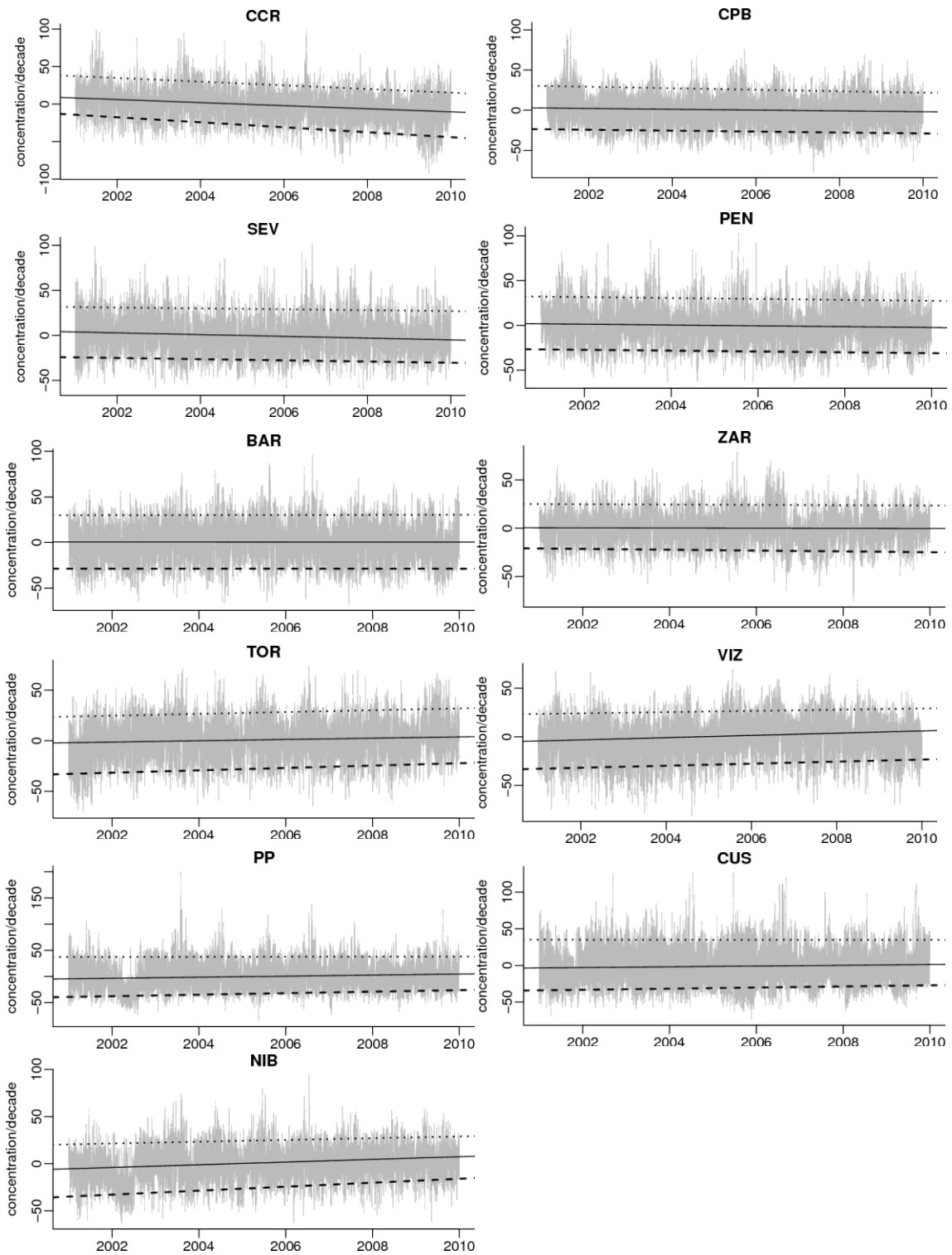


Figure4

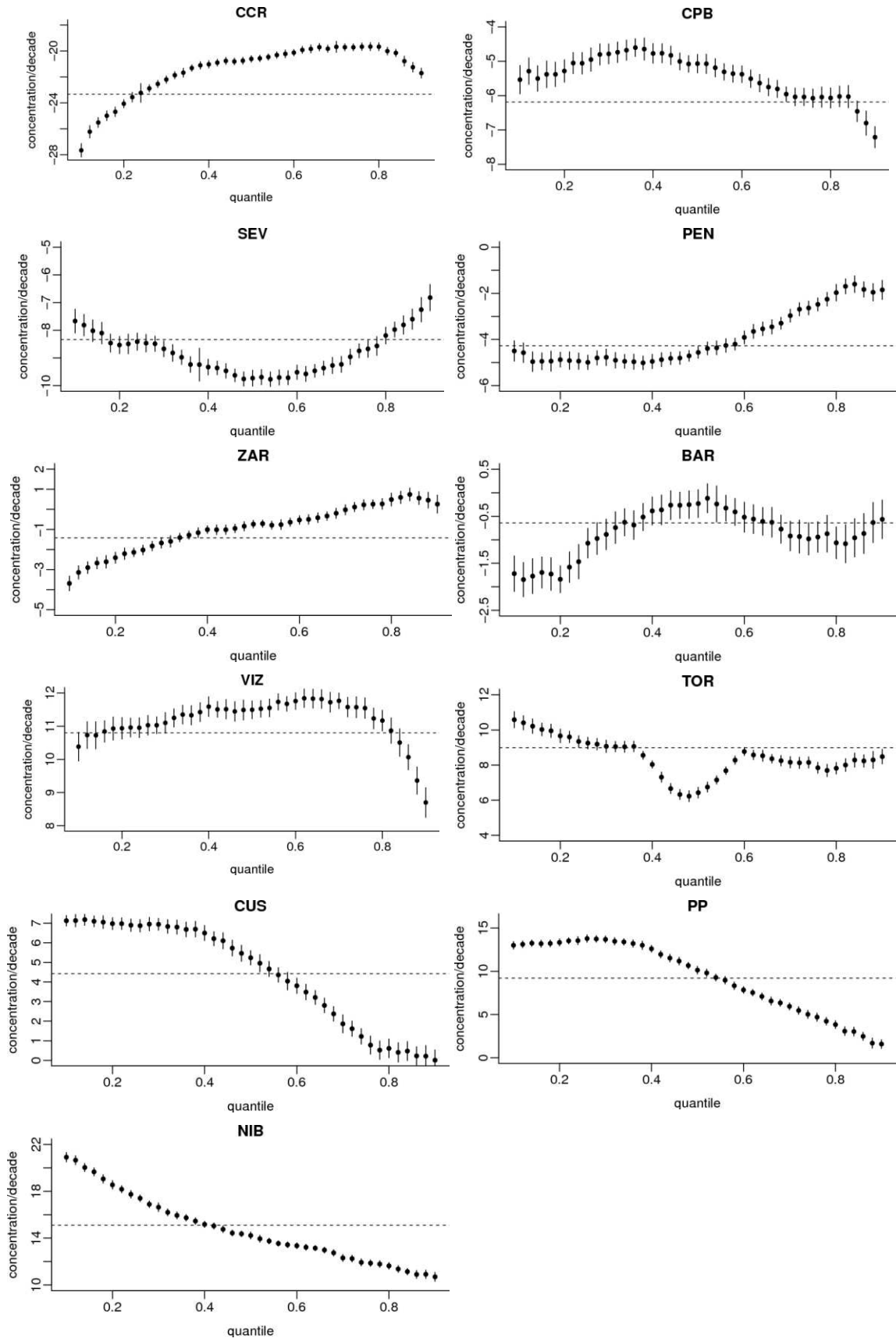


Figure5

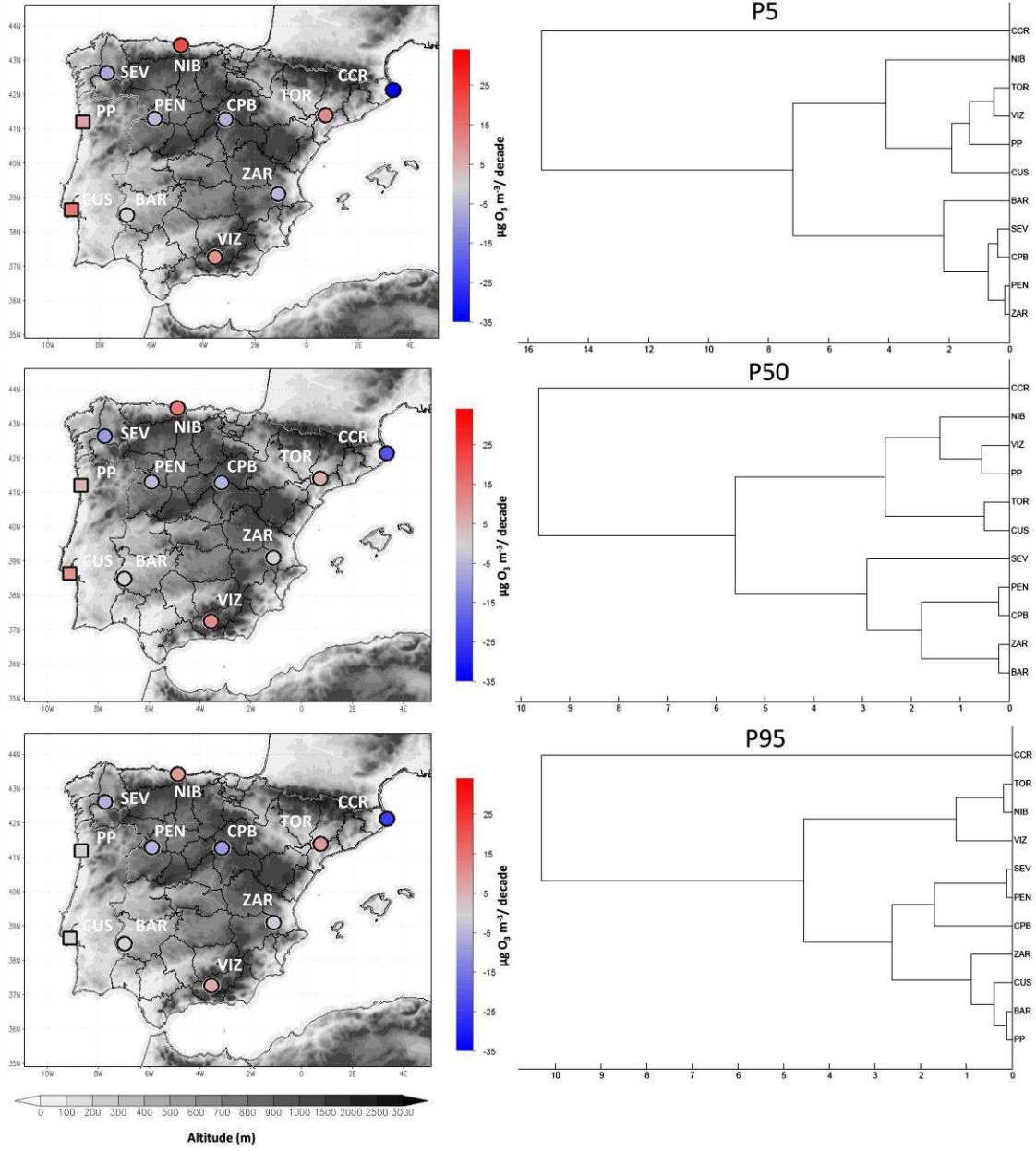


Table1[Click here to download Table: Table 1.doc](#)

Code	Station name	Country	Lat	Lon	Type	Data collection (%)	Altitude (m)
CUS	Custóias	Portugal	41.21	-8.65	Suburban	89.2%	100
PP	Paio Pires	Portugal	38.63	-9.08	Suburban	89.3%	46
VIZ	Víznar	Spain	37.23	-3.53	Rural	97.2%	1265
NIB	Niembro	Spain	43.44	-4.85	Rural	97.6%	134
CPB	Campisábalos	Spain	41.28	-3.14	Rural	95.5%	1360
CCR	Cabo de Creus	Spain	42.32	3.32	Rural	96.6%	23
BAR	Barcarrota	Spain	38.48	-6.92	Rural	97.0%	393
ZAR	Zarra	Spain	39.08	-1.10	Rural	96.8%	885
PEN	Peñausende	Spain	41.28	-5.87	Rural	91.9%	985
TOR	Els Torms	Spain	41.40	0.72	Rural	89.7%	470
SEV	O Saviñao	Spain	42.64	-7.71	Rural	85.0%	506